

Nonlinear properties of and nonlinear processing in hydrogenated amorphous silicon waveguides

B. Kuyken^{1,2,*‡}, H. Ji^{3,‡}, S. Clemmen^{4,#}, S. K. Selvaraja^{1,2}, J. Safioui⁵, H. Hu³, M. Pu³, M. Galili³, P. Jeppesen³, G. Morthier^{1,2}, S. Massar⁴, L.K. Oxenløwe³, G. Roelkens^{1,2} and R. Baets^{1,2}

¹Photonics Research Group, Department of Information Technology, Ghent University – imec, Ghent, Belgium.

²Center for Nano- and Biophotonics (NB-Photonics), Ghent University, Ghent, Belgium.

³DTU Fotonik, Technical University of Denmark, DK-2800 Kgs. Lyngby, Denmark

⁴Laboratoire d'Information Quantique (LIQ), CP 225, Université libre de Bruxelles (U. L. B.), Bruxelles B-1050, Belgium

⁵Service OPERA-Photonique, CP 194/5, Université libre de Bruxelles (U.L.B.), avenue F.D. Roosevelt 50, 1050 Brussels, Belgium

[#]now at School of Applied and Engineering Physics, Cornell University, Ithaca, New York 14853, USA

[‡]These authors contributed equally to this work

*Bart.Kuyken@intec.ugent.be

Abstract: We propose hydrogenated amorphous silicon nanowires as a platform for nonlinear optics in the telecommunication wavelength range. Extraction of the nonlinear parameter of these photonic nanowires reveals a figure of merit larger than 2. It is observed that the nonlinear optical properties of these waveguides degrade with time, but that this degradation can be reversed by annealing the samples. A four wave mixing conversion efficiency of +12 dB is demonstrated in a 320 Gbit/s serial optical waveform data sampling experiment in a 4 mm long photonic nanowire.

©2011 Optical Society of America

OCIS codes: (130.4310) Nonlinear Waveguides; (070.4340) Nonlinear optical signal processing;

References and links

1. N. Ophir, J. Chan, K. Padmaraju, A. Biberman, A. C. Foster, M. A. Foster, M. Lipson, A. L. Gaeta, and K. Bergman, "Continuous wavelength conversion of 40-Gb/s Data Over 100 nm using a dispersion-engineered silicon waveguide," *IEEE Photon. Technol. Lett.* **23**, 73–75 (2011).
2. H. Hu, H. Ji, M. Galili, M. Pu, C. Peucheret, H.C.H. Mulvad, L.K. Oxenløwe, K. Yvind, J. M. Hvam and P. Jeppesen, "Ultra-high-speed wavelength conversion in a silicon photonic chip," *Optics Express* **19**, 19886–19894, (2011).
3. I Hsieh, X. Chen, X.P. Liu, J. I. Dadap, N. C. Panoiu, C. Chou, F. Xia, W. M. Green, Y. A. Vlasov, and R. M. Osgood, "Supercontinuum generation in silicon photonic wires," *Opt. Express* **15**, 15242–15249 (2007)
4. M. A. Foster, A. C. Turner, J. E. Sharping, B. S. Schmidt, M. Lipson, and A. L. Gaeta, "Broad-band optical parametric gain on a silicon photonic chip," *Nature* **441**, 960–963 (2006).
5. H. K. Tsang, C. S. Wong, T. K. Liang, I. E. Day, S. W. Roberts, A. Harpin, J. Drake, and M. Asghari, "Optical dispersion, two-photon absorption and self-phase modulation in silicon waveguides at 1.5 μm wavelength" *Appl. Phys. Lett.* **80**, 416–418 (2002).
6. X. P. Liu, R. M. Osgood, Y. A. Vlasov, and W. M. J. Green, "Mid-infrared optical parametric amplifier using silicon nanophotonic waveguides," *Nat. Photonics* **4**, 557–560 (2010).
7. X. P. Liu, J. B. Driscoll, J. I. Dadap, R. M. Osgood, S. Assefa, Y. A. Vlasov, and W. M. J. Green, "Self-phase modulation and nonlinear loss in silicon nanophotonic wires near the mid-infrared two-photon absorption edge," *Opt. Express* **19**, 7778–7789 (2011).
8. S. Zlatanovic, J. S. Park, S. Moro, J. M. C. Boggio, I. B. Divliansky, N. Alic, S. Mookherjea, and S. Radic, "Mid-infrared wavelength conversion in silicon waveguides using ultracompact telecom-band-derived pumpsources," *Nat. Photonics* **4**, 561–564 (2010).
9. S. K. O'Leary, S. R. Johnson, P. K. Lim, "The relationship between the distribution of electronic states and the optical absorption spectrum of an amorphous semiconductor: An empirical analysis", *J. Appl. Phys.* **82**, 3334 (1997).

10. B. Kuyken, S. Clemmen, S. Selvaraja, W. Bogaerts, D. Van Thourhout, Ph. Emplit, S. Massar, G. Roelkens, R. Baets, On-chip parametric amplification with 26.5dB gain at telecommunication wavelengths using CMOS-compatible hydrogenated amorphous silicon waveguides, *Optics Letters* **36**, p.552-554 (2011).
11. S. Selvaraja, W. Bogaerts, P. Dumon, D. Van Thourhout, R. Baets, Sub-nanometer linewidth uniformity in silicon nano-photonic waveguide devices using CMOS fabrication technology, *IEEE Journal on Selected Topics in Quantum Electronics* **16**, 316 - 324 (2010).
12. S. Selvaraja, Erik Sleenckx, Marc Schaeckers, W. Bogaerts, D. Van Thourhout, P. Dumon, R. Baets, Low-Loss Amorphous Silicon-On-Insulator Technology for Photonic Integrated Circuitry, *Optics Communications* **282**, 1767-1770 (2009).
13. Y. Shoji, T. Ogasawara, T. Kamei, Y. Sakakibara, S. Suda, K. Kintaka, H. Kawashima, M. Okano, T. Hasama, H. Ishikawa, and M. Mori, "Ultrafast nonlinear effects in hydrogenated amorphous silicon wire waveguide," *Opt. Express* **18**, 5668–5673 (2010).
14. K. Narayanan, and S. F. Preble, "Optical nonlinearities in hydrogenated-amorphous silicon waveguides," *Opt. Express* **18**, 8998–9005 (2010).
15. H. K. Tsang, R. V. Penty, I. H. White, R. S. Grant, W. Sibbett, J. B. D. Soole, H. P. Leblanc, N. C. Andreadakis, R. Bhat, and M. A. Koza, "two-photon absorption and self-phase modulation in InGaAsP/InP multi-quantumwell wave-guides," *J. Appl. Phys.* **70**, 3992–3994 (1991).
16. G. P. Agrawal, *Nonlinear Fiber Optics* (Academic, San Diego, 2001) .
17. C. Koos, L. Jacome, C. Poulton, J. Leuthold, and W. Freude, "Nonlinear silicon-on-insulator waveguides for all-optical signal processing," *Opt. Express* **15**, 5976–5990 (2007).
18. H. Ji, M. Pu, M. Galili, L. K. Oxenløwe and P. Jeppesen, "Silicon based ultrafast all-optical waveform sampling," Conference of SPIE Europe Photonics Europe 2010, 7728-6, Brussels, Belgium, April (2010).
19. H. Ji, L.K. Oxenlowe, M. Galili, K. Rottwitt, P. Jeppesen, L. Gruner-Nielsen, "Fiber Optical Trap Deposition of Carbon Nanotubes on Fiber End-faces in a Modelocked Laser", CLEO'08, CtuV4, (2008).
20. H. Ji, M. Pu, H. Hu, M. Galili, L. K. Oxenløwe, K. Yvind, J. M. Hvam and P. Jeppesen, "Optical Waveform Sampling and Error-free Demultiplexing of 1.28 Tbit/s Serial Data in a Nano-engineered Silicon Waveguide," *IEEE Journal of Lightwave Technology* **29**, 426-431 (2011).
21. D. L. Staebler, C.R. Wronski, "Reversible conductivity changes in discharge-produced amorphous Si", *Appl. Phys. Lett.* **31**, 292-294, (1977).
22. M. Stutzmann, W. B. Jackson, C. C Tsai, "Kinetics of the Staebler–Wronski effect in hydrogenated amorphous silicon" *Appl. Phys. Lett.* **45**,1075-1077, (1984).

1. Introduction

The combination of both the high nonlinearity of crystalline silicon, expressed by its high nonlinear index, and the high intensities obtained in silicon photonic nanowires makes the silicon-on-insulator (SOI) platform an attractive platform for integrated nonlinear optics. Indeed, in recent years a lot of progress has been made in this field and nonlinear optical functions such as wavelength conversion [1, 2], supercontinuum generation [3] and parametric gain [4] have been demonstrated. However, the significant nonlinear absorption at telecom wavelengths [5] in crystalline silicon, the two-photon absorption (TPA), has limited the efficiency of these nonlinear devices enormously. This has led to several experiments where a pump at wavelengths above the two-photon absorption threshold wavelength of 2.2 μm was used [6-8]. Although this approach indeed lowers the nonlinear absorption in the crystalline silicon (c-Si) photonic nanowires, its use for telecommunication applications is not straightforward.

Here we demonstrate the use of highly nonlinear hydrogenated amorphous silicon photonic nanowires (a-Si:H) fabricated with CMOS compatible processes for nonlinear signal processing at telecom wavelengths. The large linear refractive index ($n \sim 3.6$) of hydrogenated amorphous silicon allows for a similar confinement as in the c-Si case. However, the higher nonlinear index of the hydrogenated amorphous silicon results in a much larger effective nonlinearity of these wires, expressed by the large real part of the nonlinearity parameter. Moreover, nonlinear absorption is only modest in the a-Si:H photonic nanowires as a result of the larger bandgap of a-Si:H compared to crystalline silicon [9].

By examining the transmission of picosecond pulses through the a-Si:H photonic nanowires, the complex nonlinear parameter was found to be $\gamma=770 - j*28 \text{ W}^{-1}\text{m}^{-1}$ at $\lambda=1550 \text{ nm}$, with j the imaginary unit. The free carrier lifetime is found to be $1.87 \pm 0.1 \text{ ns}$. In previous work these very favorable parameters were exploited in a pump/probe experiment where a four wave mixing gain of 26.5 dB was demonstrated [10]. Here we demonstrate the use of these photonic nanowires to perform an all-optical signal processing experiment. In this experiment a 320 Gbit/s serial optical data stream is successfully waveform sampled with a fourwave mixing (FWM) conversion efficiency of +12 dB, 19.5 dB better than in previous experiments in c-Si [18]. Hydrogenated amorphous silicon waveguides thus seem a very promising platform for nonlinear optics at telecommunication wavelengths. However the properties of the a-Si:H waveguides are found to degrade over time. In the final section of the paper we report measurements of this degradation, and show that it can be reversed by annealing the samples at 200°C for 30 minutes. The full realization of the potential of a-Si:H waveguides will require that this stability issue be resolved.

2. Linear and nonlinear properties of the a-Si:H photonic nanowires

The a-Si:H photonic wire waveguides were fabricated in a 200 mm CMOS pilot line at imec, Belgium [11]. First, 220 nm of a-Si:H was deposited using a low temperature Plasma Enhanced Chemical Vapor Deposition process on top of a 1950 nm surface of high-density plasma oxide on a silicon substrate. Waveguides of varying lengths (0.6 to 6 cm) were fabricated using 193 nm optical lithography and dry etching [12]. The photonic nanowires were interfaced to an optical fiber using grating couplers. The cross-section of these waveguides is $500 \times 220 \text{ nm}^2$ as can be seen in Fig 1.

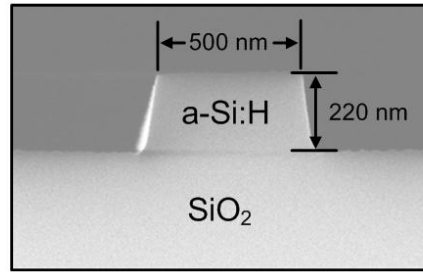


Figure 1: Cross-section of the hydrogenated amorphous silicon waveguides used in the experiments

A preliminary report on the linear and nonlinear optical properties of these waveguides was given in [10]. Here we provide a more complete characterization, as well as details of the measurements that give rise to the parameters we reported previously. For an earlier study of the nonlinear optical properties of a-Si:H waveguides we refer to [13, 14].

Using a cutback method the linear loss in the photonic nanowires was determined to be 3.6 dB/cm. Grating coupler structures are used to couple the light in and out of the chip. The incoupling loss at 1550 nm was found to be 7 dB. The group velocity dispersion has been measured to be $\beta_2=-2.0 \text{ ps}^2\text{m}^{-1}$ [10].

The nonlinear parameter of the photonic nanowires was measured by coupling in a picosecond pulse train. First, the time-averaged transmission of this picosecond pulse train (4ps, rep rate 10 MHz, center wavelength 1550 nm, spectral width 0.67 nm) in a sufficiently long (1.1 cm) photonic nanowire was measured as a function of the coupled input pulse peak power. It has been shown that the inverse of this transmission is linear as a function of the

power [15] in the low power regime, when the free carrier absorption is negligible. The inverse of the transmission is given by [15]

$$\frac{1}{T} = \exp(\alpha L) L_{eff} 2 \text{Im}(\gamma) P + \exp(\alpha L) \quad (1)$$

Here, $\text{Im}(\gamma)$ is the imaginary part of the nonlinear parameter, T is the transmission through the waveguide, L_{eff} is the effective length of the waveguide given by $L_{eff} = \frac{1 - \exp(-\alpha L)}{\alpha}$, L is the length of the waveguide and α is the linear absorption coefficient of the waveguide. A linear fit as shown in Fig. 2 reveals a value of $-28 \pm 3 \text{ W}^{-1}\text{m}^{-1}$ for the imaginary part of the nonlinear parameter. This moderate nonlinear absorption can be explained by examining the band gap of the a-Si:H, which was measured, using spectroscopic ellipsometry, to be 1.61 eV. This results in a two-photon absorption threshold wavelength of about 1540 nm.

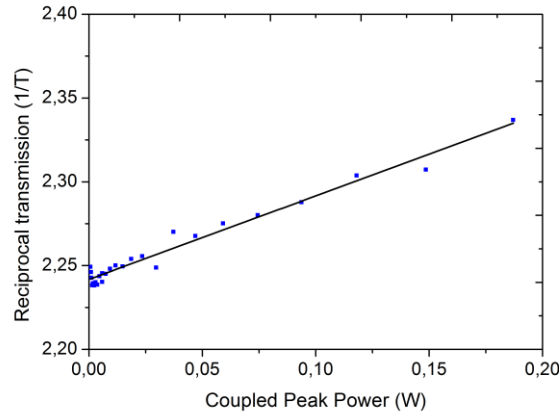


Figure 2: The reciprocal transmission as a function of the input peak power of the 4 ps pulse train. The linear fit corresponds to a nonlinear absorption coefficient of $-28 \pm 3 \text{ W}^{-1}\text{m}^{-1}$.

Next, the free carrier lifetime was extracted in a pump/probe setup. The time dependent absorption of a continuous wave (CW) laser by carriers created by a short probe by TPA is measured. As shown in Fig. 3, a low-power CW laser is combined with a high-power low repetition rate (20MHz) femtosecond laser source. The CW laser is operated at 1530 nm, while the fs laser is operating at 1550 nm such that a bandpass filter at the output only transmits the 1530 nm signal. The absorption of the low power CW signal caused by the carriers generated by the femtosecond source is measured as a function of time using a 40GHz high-speed photodiode connected to an oscilloscope. An exponential fit reveals a free carrier life time of $1.87 \pm 0.1 \text{ ns}$ as can be seen in Fig. 4.

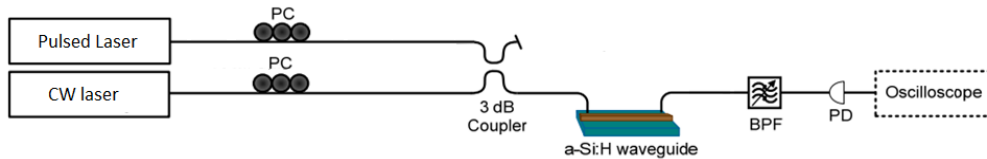


Figure 3: Experimental setup used to measure the free carrier lifetime in the hydrogenated amorphous silicon photonic nanowires.

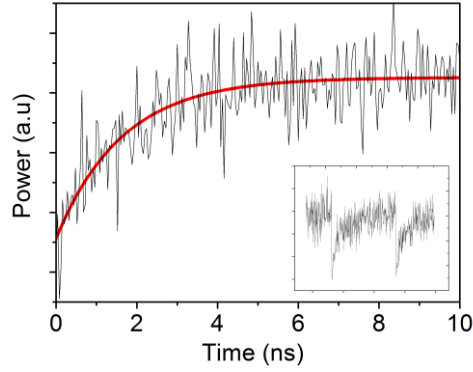


Figure 4: Oscilloscope trace of the pump/probe experiment and fit of the exponential decay of the carrier concentration, resulting in a time constant of 1.87 ± 0.1 ns.

Finally, the real part of the nonlinear parameter was measured by determining the nonlinear phase shift of the 4 ps pulses in the a-Si:H wire waveguides as a function of input power. This nonlinear phase shift was extracted from the signature [16] of the self phase modulation spectra of the pulses after having propagated through a 1.1 cm long photonic wire. These nonlinear phase shifts were compared with simulations obtained by a split step algorithm that models the pulse propagation in a nonlinear semiconductor photonic nanowire while taking into account the different forms of nonlinear absorption that occur in such a photonic nanowire. Agreement between the measured and simulated nonlinear phase shift allows the determination of the real part of the nonlinear parameter. In Fig. 5 the simulated output spectra as well as the measured output spectra are shown for a pulse peak power of 1.4, 2.9, 4.6 and 7.3 W. This method shows that the real part of the nonlinear parameter is $770 \pm 100 \text{ W}^{-1} \text{ m}^{-1}$. By comparing the real and imaginary part of the nonlinear photonic nanowire a figure of merit (FOM) [17] can be defined as

$$FOM = -\frac{\text{Re}(\gamma)}{4\pi \text{Im}(\gamma)} \quad (2)$$

The extracted FOM of 2.2 at $\lambda=1550\text{nm}$ for a-Si:H waveguides is almost four times higher than value obtained in c-Si photonic nanowires [17].

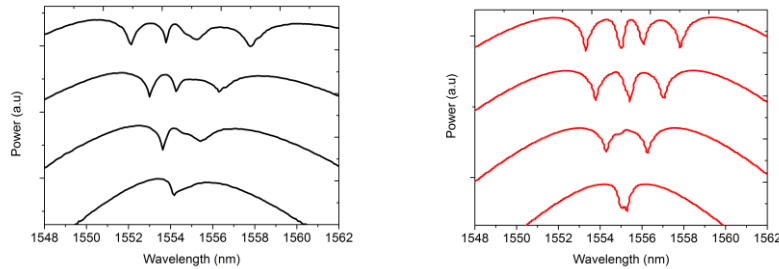


Figure 5: The simulated output spectra of a 4ps FWHM pulse train (right) and measured output spectra (left) for a coupled input peak power of 1.4, 2.9, 4.6 and 7.3W after propagation through a 1.1 cm long a-Si:H photonic nanowire.

3. Optical Waveform Sampling of a 320 Gbit/s Serial Data Signal

To demonstrate the ultrafast large nonlinear response of the a-Si:H photonic nanowires, an optical waveform sampling experiment was performed in a 4 mm long waveguide. The setup of this experiment is shown in Fig. 6.

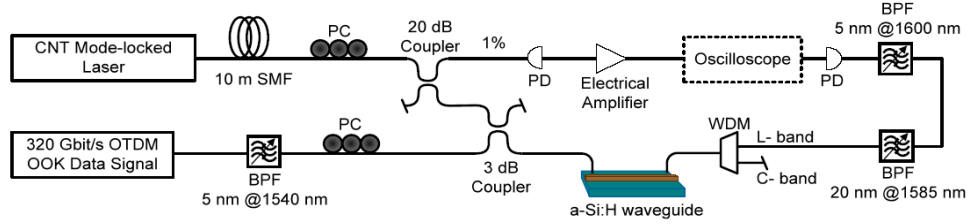


Figure 6: Experimental setup used in the 320 Gbit/s waveform sampling experiment

A fiber ring mode-locked laser is used as the sampling source, which uses a 30 cm erbium-doped fiber as gain medium and a carbon nanotubes (CNT) mode-locker [18]. The generated sampling pulses have a repetition rate of 16.3 MHz and a sech pulse shape with a FWHM width of ~ 710 fs, measured using an autocorrelator directly at the laser output. The central wavelength of the pulses lies at 1558 nm and the 3-dB spectral bandwidth is 4 nm. The sampling pulses are broadened to 1.4 ps by adding 10 m single mode fiber (SMF) to avoid broadening by self phase modulation in the a-Si:H photonic nanowires. Using the Optical Time Division Multiplexing (OTDM) technique, a 320 Gbit/s serial data stream signal is generated. An erbium glass oscillator (ERGO) optical pulse source generates a 10 GHz pulse train at 1550 nm with 2 ps FWHM pulses. After amplification in an EDFA, the 10 GHz data pulses are sent into a dispersion-flattened highly nonlinear fiber (DF-HNLF) to broaden the spectrum. Then a 5 nm bandpass filter is used to filter out part of the spectrum. The pulse width of the 10 GHz pulses is compressed to 1 ps in this way. A Mach-Zehnder modulator encodes a 10 Gbit/s on-off keying (OOK) data sequence (PRBS 2^7-1) on the pulse train and the 10 Gbit/s data signal is multiplexed to 320 Gbit/s by a passive fiber delay and polarization maintaining multiplexer (MUX). The 320 Gbit/s OTDM OOK data signal is coupled into the a-Si:H waveguide together with the sampling pulse train. The average data signal power and sampling pulse train power before coupling into the a-Si:H waveguide is 5 dBm and -5 dBm respectively. In the a-Si:H waveguide, FWM will take place when the sampling pulses (pump) overlap with the data pulses (signal) and generate a new FWM product (idler). After the a-Si:H waveguide, the FWM product is selected by L-band filters and directly detected using a high sensitivity photo-detector (with 200 MHz bandwidth). A tunable optical delay is inserted in the cavity of the sampling laser to fine tune the cavity length so that the repetition rate can be adjusted in a small range, this means in turn that the temporal offset, Δt , between sampling and signal pulses can be adjusted. This tunable temporal offset provides a simple synchronization scheme by only using the free running sampling pulses itself as a gate trigger for the oscilloscope [19].

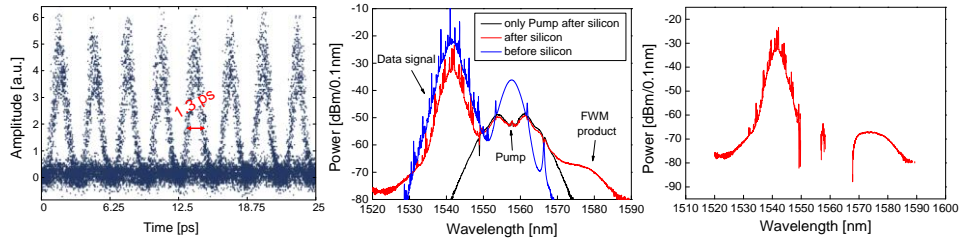


Figure 7: (Left) Sampled eye-diagram of the 320 Gbit/s serial data signal using the a-Si:H based optical sampling system, (Middle) Measured optical spectra before and after the a-Si:H waveguide, (Right) Spectrum of data signal and FWM product at output of waveguide when subtracting the pump.

The measured spectra in the experiment are shown on Fig. 7 (middle). The output spectrum is broadened by SPM in the a-Si:H photonic nanowires. Fig. 7 (Right) shows the spectra of the data signal and FWM product at the output of the waveguide. The output power of the data signal and FWM product are integrated spectrally and measured to be $P_{data_out} = -14.5$ dBm and $P_{FWM_out} = -44$ dBm, respectively. The conversion efficiency, defined as the ratio between the FWM product power just before it is coupled out from the a-Si:H waveguide and the data signal power coupled into the a-Si:H waveguide, can be expressed as

$$\eta = (P_{FWM_out} + l_{coupling}) - (P_{data_out} + l_{coupling} + l) \quad (3)$$

where $l_{coupling}$ is the coupling loss between fiber and waveguide (expressed in dB), and l is the propagation loss of the a-Si:H waveguide (1.5 dB for the 4mm long waveguide). When the duty cycle of the sampling pulse train (-43 dB) is taken into account, the intrinsic conversion efficiency η is found to be +12 dB. This is an improvement of almost 19.5 dB as compared to a similar optical sampling system based on c-Si [20], where the intrinsic conversion efficiency was found to be merely -7.5 dB.

4. Material degradation

The strong nonlinearity in the a-Si:H manifests itself through strong modulation instability [16]. Evidence of modulation instability, the four wave mixing process where white background noise gets amplified, is shown in Fig. 8(a). At the output of the photonic nanowire the spectrum of the pulse train shows sidelobes, resulting from the parametric amplification of the background noise. The pulses used in these experiments were 4-ps FWHM with a coupled peak power of 5.2 W and had a repetition rate of 10 MHz. The experiment shows that the amplification becomes weaker over time resulting in weaker modulation instability side lobes. The observed decrease of the parametric amplification is believed to be the result of material degradation, probably originating from the Staebler-Wronski effect [21], well known in the a-Si solar cell community. Shortly after the first demonstration of thin-film amorphous silicon solar cells it was shown that these cells were not stable and that their efficiency decreases over time [21]. It was found [22] that this results from the degradation of the material, due to a process in which electron-hole pairs created by energetic photons recombine in the material.

When the hydrogenated amorphous silicon photonic nanowires are exposed to telecom wavelengths it is unlikely that a substantial number of electron-hole pairs can be created by single photon absorption. However when high power pulses enter the photonic nanowires free carriers are created due to the presence of two-photon absorption. These free carriers can degrade the material following the Staebler Wronski mechanism.

It was however demonstrated in amorphous silicon solar cells that the material can be restored to its original state by thermally annealing the sample. The same occurs for a-Si:H

photonic chips. Here, the sample was heated at 200 °C for 30 minutes and the effects of the degradation were reversed. Even after four iterations in which the sample is sequentially exposed to the bright pulses (4 ps, 5.2 W coupled peak power, 10 MHz rep rate) for 40 minutes and thermally annealed for half an hour the material was brought again to its original state. This is shown in Fig. 8 (b). In this figure the peak power in the side lobes is plotted versus time. Even after four iterations the curve shows no deviation from the first iteration.

It is also important to note that the nonlinear parameters from the waveguide were extracted after 30 minutes of exposure, when the material is in a quasi steady state.

Given that the bandgap of the a-Si:H layers can be altered by modifying the fabrication process, the two-photon absorption can be lowered by increasing the bandgap in differently processed a-Si:H thin films. This would allow for a stable highly nonlinear platform. Such material optimization is currently being carried out but lies outside the scope of the present paper.

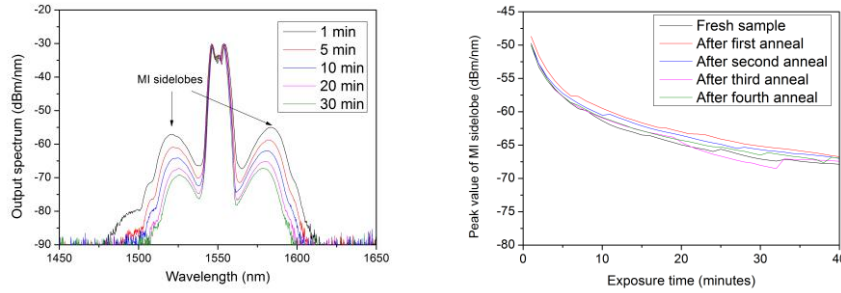


Figure 8: The modulation instability (MI) side lobes decrease over time (left) when the sample is exposed to intense light. The optical pulses in this experiment had their central wavelength at 1550 nm, had a repetition rate of 10 MHz and a FWHM of 4ps. The right figure shows the peak value of the right MI side lobe versus time, after successive thermal annealing steps of the sample at 200°C for 30 minutes.

4. Conclusions

The linear and nonlinear coefficients from the hydrogenated amorphous silicon photonic nanowires were extracted in this paper. The linear absorption was found to be 3.6 dB/cm while the nonlinear parameter was found to be $\gamma = 770 - j*28 \text{ W}^{-1}\text{m}^{-1}$ after exposing the waveguides for 30 minutes. This results in a figure of merit larger than 2. The carrier lifetime was estimated to be $1.87 \pm 0.1 \text{ ns}$. The potential of the a-Si:H photonic nanowires for all-optical nonlinear processing was demonstrated by a 320 Gbit/s waveform sampling experiment. The intrinsic FWM conversion efficiency in this experiment was +12 dB. This is an improvement of 19.5 dB as compared to similar sampling experiments in c-Si [19]. The degradation of the hydrogenated amorphous silicon layers is discussed. This degradation is presumably caused by a process similar to the Staebler-Wronski effect in amorphous silicon solar cells. As with the Staebler-Wronski effect in amorphous silicon cells, the degradation can be reversed by thermally annealing the sample. This was demonstrated by heating the sample for half an hour at 200 °C. Improving the stability, for example by increasing the bandgap, could make the hydrogenated amorphous silicon photonic nanowires the platform for nonlinear integrated optics in the telecommunication wavelength range.

Acknowledgements

B. Kuyken acknowledges the Flemish Research Foundation, Vlaanderen for a doctoral fellowship. This work was partly carried out in the framework of the Methusalem “Smart Photonic Chips,” FP7-ERC-INSPECTRA and FP7-ERC-MIRACLE. We acknowledge

support by the Interuniversity Attraction Poles Photonics@be Program (Belgian Science Policy) under grant IAP6-10.